DOI: 10.1002/chem.201002577

VIP

Aromatic Hydroxylation at a Non-Heme Iron Center: Observed Intermediates and Insights into the Nature of the Active Species

Olga V. Makhlynets and Elena V. Rybak-Akimova*[a]

Abstract: Mechanism of substrate oxidations with hydrogen peroxide in the presence of a highly reactive, biomimetic, iron aminopyridine complex, $[Fe^{II}(bpmen)(CH_3CN)_2][ClO_4]_2$ (**1**; bpmen = *N*,*N*′-dimethyl-*N*,*N*′-bis(2-pyridylmethyl)ethane-1,2-diamine), is elucidated. Complex **1** has been shown to be an excellent catalyst for epoxidation and functional-group-directed aromatic hydroxylation using H_2O_2, although its mechanism of action remains largely unknown.[1,2] Efficient intermolecular hydroxylation of unfunctionalized benzene and substituted benzenes with H_2O_2 in the presence of **1** is found in the present work. Detailed mechanistic studies of the formation of iron(III)–phenolate products are reported. We have identified, generated in high yield, and experimentally characterized the key $Fe^{III}(OOH)$ intermediate ($\lambda_{max} = 560$ nm, rhombic EPR signal with $g = 2.21$, 2.14, 1.96) formed by **1** and H_2O_2. Stopped-flow kinetic studies showed that $Fe^{III}(OOH)$ does not directly hydroxylate the aromatic rings, but undergoes rate-limiting self-decomposition producing transient reactive oxidant. The formation of the reactive species is facilitated by acid-assisted cleavage of the O–O bond in the iron–hydroperoxide intermediate. Acid-assisted benzene hydroxylation with **1** and a mechanistic probe, 2-Methyl-1-phenyl-2-propyl hydroperoxide (MPPH), correlates with O–O bond heterolysis. Independently generated Fe^{IV}=O species, which may originate from O–O bond homolysis in $Fe^{III}(OOH)$, proved to be inactive toward aromatic substrates. The reactive oxidant derived from **1** exchanges its oxygen atom with water and electrophilically attacks the aromatic ring (giving rise to an inverse H/D kinetic isotope effect of 0.8). These results have revealed a detailed experimental mechanistic picture of the oxidation reactions catalyzed by **1**, based on direct characterization of the intermediates and products, and kinetic analysis of the individual reaction steps. Our detailed understanding of the mechanism of this reaction revealed both similarities and differences between synthetic and enzymatic aromatic hydroxylation reactions.

Keywords: hydrogen peroxide · hydroxylation · iron · kinetics · oxidation

Introduction

Development of regio- and stereoselective catalytic oxidation of organic substrates is an important goal for organic synthesis. Biomimetic oxidations are particularly attractive, because they rely on cheap, nontoxic reactants (usually, O_2 or H_2O_2 as oxidants, and Fe, Cu, or Mn complexes as catalysts). Developing the chemistry of non-heme iron oxidations proved to be intellectually rewarding and productive, and impressive recent progress includes crystallization and characterizations of several high-valent iron intermediates,[3–5] as well as discovery of synthetically useful, regioselective epoxidations and hydroxylations catalyzed by biomimetic iron complexes.[6] One of the most successful olefin epoxidation catalysts is an iron(II) complex of a tetradentate aminopyridine ligand: $[Fe^{II}(bpmen)(CH_3CN)_2](ClO_4)_2$ (**1**; bpmen = *N*,*N*′-dimethyl-*N*,*N*′-bis(2-pyridylmethyl)ethane-1,2-diamine) that converts olefins into epoxides with high selectivity and efficiency with hydrogen peroxide as the oxidant.[1] It has also been shown to be a selective catalyst for aliphatic C–H oxidation,[7] and regioselective aromatic hydroxylation.[2,8] Over the past decade the identity of the reactive intermediate in the catalytic oxidation promoted by **1** became a subject of interest. Although there is no general mechanism for a non-heme systems that activate oxygen,[9] several intermediates, including $Fe^{III}(OOH)$, Fe^{IV}=O, and Fe^{V}=O, have been proposed as active species in catalytic cycles of enzymes and enzyme models.[6,10] A generally ac-

[a] O. V. Makhlynets, Prof. Dr. E. V. Rybak-Akimova
Department of Chemistry, Tufts University
62 Talbot Ave., Medford, MA 02155 (USA)
Fax: (+1) 617-627-3443
E-mail: erybakak@tufts.edu

Supporting information for this article is available on the WWW under http://dx.doi.org/10.1002/chem.201002577.

cepted scheme of the reaction of **1** and H_2O_2 includes formation of the $Fe^{III}(OOH)$ intermediate that undergoes heterolytic O–O bond cleavage and yields active Fe^{V}=O (Scheme 1B). The recent progress in understanding of the mechanism of oxygen activation at **1** was based on indirect evidence and no reaction intermediates were reliably characterized, although Talsi et al. detected $Fe^{III}(OOH)$ by EPR spectroscopy at −60 °C in very low yield.[11] In this work we followed rapid reactions of **1** with H_2O_2 and found conditions to generate $Fe^{III}(OOH)$ in a high yield and characterized this intermediate by EPR spectroscopy. Furthermore, we have tested the reactivity of this novel intermediate.

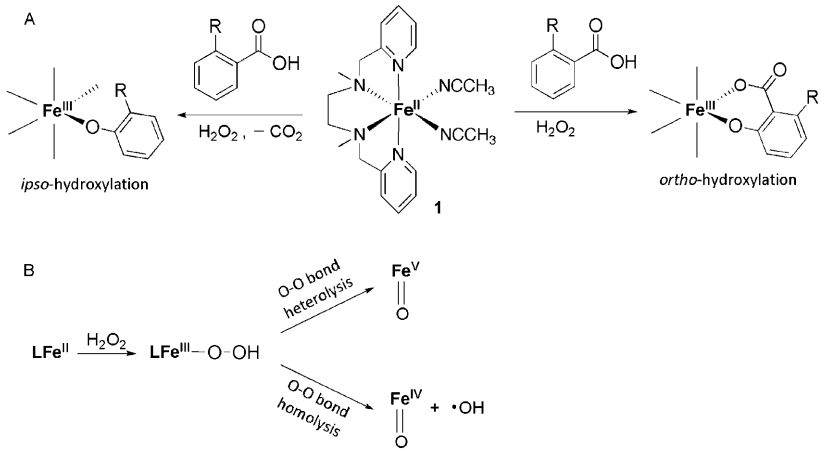

Scheme 1. A) *ortho*- and/or *ipso*-hydroxylation of benzoic acids with H_2O_2 promoted by **1**; B) possible reactivity modes of $Fe^{III}(OOH)$ intermediate: $Fe^{III}(OOH)$ can either directly transfer oxygen to substrate, or decompose into a high-valent iron–oxo species that reacts with the substrate.

Aromatic hydroxylation presents an excellent opportunity to gain detailed insights into the reactivity of complex **1**. We have recently reported that the hydroxylation of the aromatic ring of substituted benzoic acids occurs exclusively in the vicinity of the anchoring carboxylate functional group leading to *ortho*- or *ipso*-hydroxylated products (Scheme 1A).[2] This carboxylic acid directed regioselectivity implies involvement of a highly reactive, metal-based oxidant that attacks the aromatic ring next to the directing group. One specific question that needs to be addressed is the role of carboxylic acid functionality in regioselective aromatic hydroxylations. In addition to being an anchoring, directing group that coordinates to the metal center of **1**, carboxylic acid can also serve as a source of protons. Other carboxylic acids, such as acetic acid, were used to improve performance of **1** as catalyst of olefin epoxidation and aliphatic C–H oxidation.[1,7] Que and co-workers proposed that coordinated carboxylic acid promotes O–O bond heterolysis of the $Fe^{III}(OOH)$ with formation of an Fe^{V}=O species.[12] In order to better understand the mechanism of oxidations with hydrogen peroxide promoted by **1**, we now report a detailed study of hydroxylation of non-coordinating aromatic hydrocarbons, and the effects of externally added carboxylic acids on the rates and mechanisms of aromatic hydroxylation. This approach, which places two critical components of aromatic hydroxylation in separate molecules, decouples the reactivity of the aromatic rings from the reactivity of carboxylic acids. Our kinetic studies and isotope-labeling experiment show that $Fe^{III}(OOH)$ is not the active oxidant in hydroxylation reaction, but it produces the reactive high-valent species in the rate-limiting step. The reactive species formation is facilitated by protonation of the terminal oxygen in $Fe^{III}(OOH)$, which leads to heterolytic cleavage of the O–O bond and formation of a putative Fe^{V}=O species.

Results and Discussion

Hydroxylation of benzene by hydrogen peroxide in the presence of 1: The reactivity of **1** in hydroxylation of aromatic hydrocarbons with hydrogen peroxide at room temperature was explored in the present work. Benzene reacts with hydrogen peroxide in the presence of **1** to form a blue species (λ_{max}=650 nm), which later decays (Figure 1). Quenching the reaction followed by a workup (see Experimental Section) and GCMS identified the oxidation product as phenol. Coordination of the deprotonated phenol to iron(III) in the oxidized form of **1** generates colored products, similarly to the formation of intensely colored salicylates upon hydroxylation of benzoic acids promoted by **1**.[2,8] Screening and optimization of reaction conditions revealed that the best yields of hydroxylated products (phenolates) were obtained in ace-

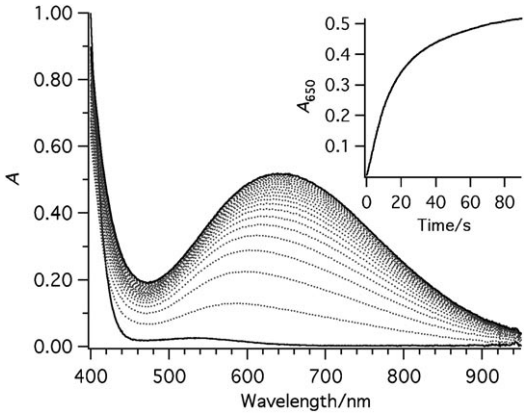

Figure 1. UV/Vis spectral changes for the reaction of **1**, benzene and H_2O_2 in acetonitrile at 20 °C ([**1**] = 0.5 mM, [H_2O_2] = 5 mM, 200 equiv of benzene vs. **1**). Solid lines represent spectra of **1** (time 0 s) and a product [(bpmen)Fe^{III}-OPh]$^{2+}$ (run time 90 s). Inset: kinetic trace at 650 nm showing accumulation of [(bpmen)Fe^{III}-OPh].

tonitrile at room temperature, with excess of H_2O_2 (10 equiv vs. **1**) and benzene (300 equiv vs. **1**). Strongly coordinating solvents, such as methanol and DMSO, suppress benzene hydroxylation promoted by **1**, presumably due to the substitution of labile acetonitrile in the coordination sphere of iron and blocking an access of the oxidant and the substrate to the iron center. Excess of hydrogen peroxide dramatically improves the conversion of benzene into phenol, but also causes subsequent oxidation of phenol into dihydroxybenzenes (Figure S1 in the Supporting Information). We utilized small excess of hydrogen peroxide (3 equiv) for kinetic and deuterium retention studies, for which formation of dihydroxybenzene would make interpretation of results more difficult, and larger quantities (10 equiv) to characterize metal-based intermediates using EPR spectroscopy and stopped-flow spectrophotometry. Time-resolved UV/Vis and GCMS data show that hydroxylation reaction is complete in 5 min; GC and spectrophotometric yields of phenol match closely (Figures S2 and S3 in the Supporting Information).[13] Although the reaction is rapid and high-yielding, efficient catalysis is precluded by strong coordination of the phenolate products to the iron(III) center.

The scope of the hydroxylation reaction: Although general, aromatic hydroxylation catalyzed by **1** is sensitive to the nature of substrate. Without an anchoring group it affords a mixture of *o*-, *m*- and *p*-substituted phenols (Scheme 2 and Table S1 in the Supporting Information). Sterically hindered substrates (e.g., 1-*tert*-butyl-3,5-dimethylbenzene) and substrates with strong electron-withdrawing groups (e.g., nitrobenzene) give very low yield of phenol (Table S1 in the Supporting Information).

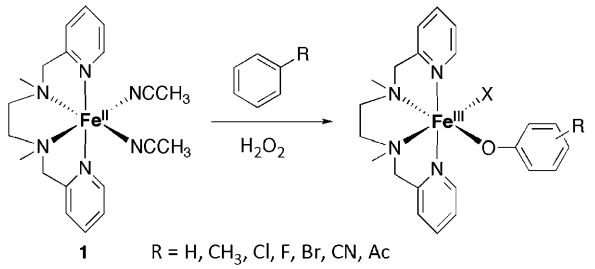

Scheme 2. The scope of hydroxylation reaction.

The **1**/H_2O_2 system favors aromatic hydroxylation over hydroxylation of methyl group (phenols/benzyl alcohol ≈11:1 in toluene hydroxylation). However, aliphatic chain is preferentially hydroxylated when a methylene group is available (Figure S4 in the Supporting Information). Additions of acetic acid can modulate both the activity and the selectivity of oxidation reactions mediated by **1** and related aminopyridine iron complexes. For example, olefin epoxidation is strongly favored in the presence of acetic acid, while dihydroxylation dominates in acid-free reactions.[1,12] Similarly, we observed alteration of ethylbenzene hydroxylation in the presence of acetic acid: the yield of aromatic hydroxylation product increased, while the yield of methylene hydroxylation product decreased (Figure S4 in the Supporting Information). Presumably, the nature of the reactive intermediates and/or their reactivity can be altered in presence of carboxylic acids.

Both steric and electronic effects in aromatic hydroxylation by **1**/H_2O_2 differ from non-selective reactivity of hydroxyl radicals (for example, nitrobenzene affords nitrophenols in reactions with HO$^{\bullet}$ generated by photolysis of α-azohydroperoxide).[14] Moreover, hydroxylation of chlorobenzene with **1**/H_2O_2 in the presence of a radical trap (galvinoxyl radical, ≈1 equiv vs. **1**) did not affect the yield of phenol. These observations suggest involvement of metal-based intermediates in non-radical aromatic hydroxylation with **1**/H_2O_2. A metal-based intermediate was also implicated in a related aromatic hydroxylation of benzoic acids with **1**/H_2O_2.[2]

Kinetic and mechanistic studies of benzene hydroxylation: The formation of a phenolate upon mixing of **1** with benzene/H_2O_2 appears as a two-exponential process (Figure S5 in the Supporting Information). The effective pseudo-first-order rate constants k_{1obs} and k_{2obs} do not depend on concentration of **1** indicating the reaction's first-order in **1**. The first step of hydroxylation reaction was found to be first order in H_2O_2, while the second step is independent of [H_2O_2] (Figure S6 in the Supporting Information). Neither k_{1obs} nor k_{2obs} depend on substrate concentration (Table S2 in the Supporting Information), but the spectroscopic yield of phenol is proportional to the concentration of H_2O_2 (Figure S5 in the Supporting Information) and benzene. Furthermore, the rate of hydroxylation is not affected by the nature of substrates (Table S3 in the Supporting Information), but the spectroscopic yields of phenolate products under otherwise identical conditions generally increase for electron-rich substrates (Figure S7 in the Supporting Information). These results suggest a mechanistic hypothesis: the first reaction step affords an intermediate that decomposes in a subsequent rate-limiting step producing an active oxidant. To test this assumption, we examined individual reaction steps and identified reactive intermediates.

Reaction of complex 1 with H_2O_2—formation of the Fe^{III}-(OOH) intermediate: Stopped-flow studies of the direct reaction between **1** and H_2O_2 under optimal hydroxylation conditions (room temperature, acetonitrile) identified a new purple intermediate with $\lambda_{max}=560$ nm (species **2**, Figure 2) that is short-lived at room temperature (half-life time 30 s). The optical spectrum of **2** is similar to the spectra of known mononuclear Fe^{III}(OOH) complexes, which typically have an intense band at ≈500–550 nm ($\varepsilon \approx 1000\,M^{-1}cm^{-1}$).[15–22] Fe^{III}(OOH) was proposed to be a plausible reaction intermediate in reactions of **1** with H_2O_2;[8,12,23] however, owing to the low yield of the intermediate (<3%) its absorption spectrum could not be recorded.[11] Our stopped-flow experiments confirmed that the addition of hydrogen peroxide to

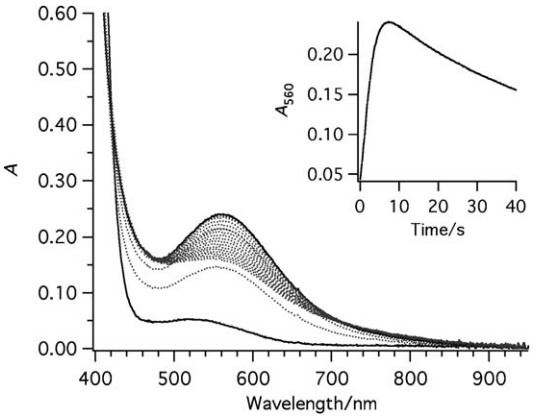

Figure 2. Time-resolved UV/Vis spectra of the $Fe^{III}(OOH)$ formation at 20 °C in acetonitrile ([**1**] = 1 mM, $[H_2O_2]$ = 10 mM). Inset: kinetic trace at 560 nm. Solid lines are spectra of **1** and $Fe^{III}(OOH)$ at its maximum formation.

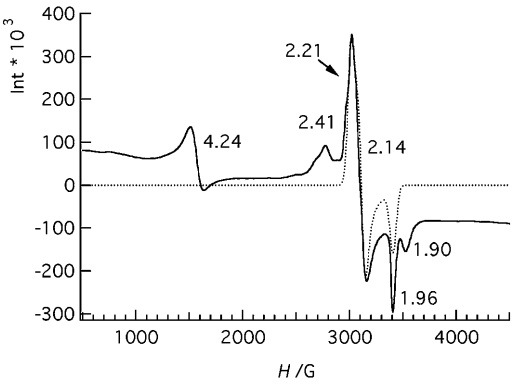

Figure 3. EPR spectrum (120 K) of $Fe^{III}(OOH)$ in acetonitrile. 25% yield of $Fe^{III}(OOH)$ vs. initial concentration of iron was determined using $Cu(ClO_4)_2$ as an external standard. Signals at 2.41 and 1.90 correspond to **3**, which accompanies **2** at all temperatures.

1 at lower temperatures (−80 to −30 °C) affords only yellow species **3**, and no purple species was detected (Figure S8 in the Supporting Information). Unlike the majority of reactive intermediates, that are generated in higher yields at low temperature, the yield of **2** at the time of its maximum accumulation increased as temperature increased from −20 °C to +20 °C (Figure S9 in the Supporting Information), although decomposition of **2** also accelerated with temperature. The transient nature of this intermediate may have prevented its observation and trapping in the past.

The plot of the observed rate constants versus hydrogen peroxide concentration under pseudo-first-order conditions (ca. 10-fold excess H_2O_2 with respect to **1**) is a straight line with a nearly zero intercept (Figure 5,S10), indicating first-order in H_2O_2 and the overall mixed second-order for the formation of $Fe^{III}(OOH)$:

$$v(Fe^{III}OOH\ \text{formation}) = k[\mathbf{1}][H_2O_2]$$

Relatively high activation enthalpy ($\Delta H^{\neq} = 55.0\ kJ\,mol^{-1}$, Figure S11 in the Supporting Information) and large negative activation entropy ($\Delta S^{\neq} = -29.3\ J\,mol^{-1}\,K^{-1}$, Figure S12 in the Supporting Information) are consistent with a bimolecular rate-limiting step, although the activation parameters for a multistep conversion of **1** into **2** are likely to be composite values, and straightforward interpretation may be misguided.

Intermediates **2** and **3** were characterized by EPR spectroscopy and mass spectrometry. The main product of the reaction between **1** and H_2O_2 at −30 °C was a low-spin iron(III) species (**3**) with g = 2.41, 2.17 and 1.90 (Figure S13 in the Supporting Information). Most likely, an oxidation of **1** without subsequent coordination of hydroperoxide occurs under these conditions. Freezing the reaction solution at the maximum accumulation of **2** (room temperature, Figure 2) gives a sample with two species: g values 2.21, 2.14, 1.96 and 2.41, 2.17 and 1.90 (Figure 3); the additional signal at 4.24 belongs to a small amount of a high-spin rhombic iron(III) product. The set of signals with g = 2.21, 2.14, 1.96 (ca. 30% of total iron) is typical of low-spin iron(III)–hydroperoxo species (with characteristic range of g values of 1.93–2.26)[24] and thus is assigned to **2**. Simultaneous formation of two low-spin iron(III) species has been previously observed when Fe^{II}–BLM (BLM = bleomycin) reacted with O_2,[25,26] first signals of $Fe^{III}(OOH)$–BLM grew in (g = 2.26, 2.17 and 1.94) and then the decay product Fe^{III}–BLM accumulated (g = 2.45, 2.18 and 1.89). Complexes with aminopyridyl ligands similar to bpmen (L) also react with hydrogen peroxide to produce a mixture of low-spin iron species (Table S4 in the Supporting Information); one set of signals in EPR spectrum corresponds to $Fe^{III}(OOH)$ and the other set was assigned to $[Fe^{III}(L)X]^{n+}$ (n = 2 or 3; X = Cl, OH, H_2O, OMe, HOMe),[18,19,27] which presumably serves as a presursor to $Fe^{III}(OOH)$. Taken together, the EPR spectroscopy and the stopped-flow UV/Vis data indicate that **2** is an $Fe^{III}(OOH)$ species. This conclusion is supported by the observed ESI-MS of **2**, which shows peaks at m/z = 425, 442, 456, and 481 consistent with ions $[Fe(bpmen)+ClO_4]^+$, $[Fe(bpmen)(OH)+ClO_4]^+$, $[Fe(bpmen)(OMe)+ClO_4]^+$, $[Fe(bpmen)(OOH)+Na+ClO_4]^+$ respectively (Figure S14 in the Supporting Information).

To directly probe whether $[Fe^{III}(bpmen)(OOH)(CH_3CN)]^{2+}$ (**2**) is involved in benzene hydroxylation, we added this substrate to a pre-generated **2**, and observed the formation of a blue Fe^{III}–phenolate complex (Figure 4). However, this experiment does not prove that the intermediate **2** itself attacks benzene; additional kinetic studies (detailed below) were performed in order to further probe the reactivity of **2**.

$Fe^{III}(OOH)$ reactivity pathways and effect of acetic acid: Iron–hydroperoxide is often considered to be a reaction intermediate in nonheme iron systems[15,16,28,29] that may either directly transfer an oxygen atom to the substrate, or decompose into a high-valent iron–oxo species that reacts with the substrate.[12,30,31] However, the experimental data on the reactivity of $Fe^{III}(OOH)$ are limited, and hardly support a uniform view on their ability to directly oxidize substrates. For example, Nam et al. tested the ability of several synthetic

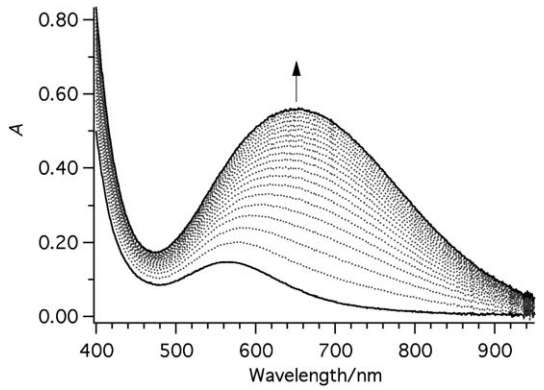

Figure 4. Time-resolved UV/Vis spectra of the reaction of Fe^{III}(OOH) with benzene in acetonitrile at 20 °C ([**1**] = 0.5 mM, [H_2O_2] = 5 mM, 200 equiv of benzene vs. **1**). Solid lines represent spectrum of **2** (λ_{max} = 560 nm) at its maximum formation (age time 7 s) and a spectrum of a product [(bpmen)Fe^{III}-OPh] (λ_{max} = 650 nm, run time 80 s).

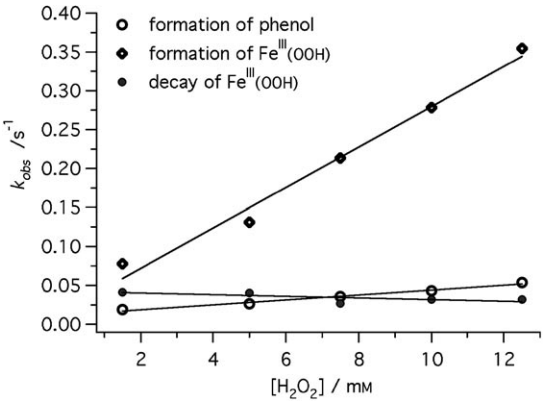

Figure 5. Rates of formation of phenol, Fe^{III}(OOH) and decay of Fe^{III}-(OOH) in acetonitrile at 20 °C as a function of H_2O_2 concentration. Rate constant of hydroxylation was determined from a single mixing experiment, in which **1** was mixed with benzene and H_2O_2 ([**1**] = 0.5 mM, 300 equiv benzene vs. **1**). Kinetic traces at 650 nm were fitted in Kinetic Studio program using A→B→C model. Formation and decay of Fe^{III}-(OOH) was monitored at 560 nm after **1** (0.5 mM) was mixed with H_2O_2; kinetic traces at 560 nm were fitted using A→B→C model, in which the first process represents formation of Fe^{III}(OOH) and the second process is a decay of Fe^{III}(OOH).

iron–hydroperoxo complexes to oxidize sulfides or olefins, and concluded that this intermediate is a sluggish oxidant.[32] On the other hand, Solomon et al. reported that Fe^{III}(OOH) in activated bleomycin (ABLM) directly attacks DNA.[26]

Kinetic data for benzene hydroxylation compared with kinetics of the reaction of **1** with H_2O_2 (Figure S15 in the Supporting Information) suggest that **2** does not attack aromatic ring, but decomposes into another, more active intermediate (Scheme 5). The rate constant of the formation of Fe^{III}-(OOH) from **1** and H_2O_2 is comparable to the observed rate constant of the first process in benzene hydroxylation studies (k_{1obs}, Figure S6 in the Supporting Information). Both rate constants are directly proportional to [H_2O_2]. Since absorption bands of Fe^{III}(OOH) and Fe^{III}–phenolates (λ_{max} = 560 and 650 nm, respectively) partially overlap, we observe a two exponential process when **1** is mixed with benzene/H_2O_2, in which k_{1obs} corresponds to the formation of Fe^{III}-(OOH) (Figure 5) and k_{2obs} is attributed to the hydroxylation of benzene. The rate constant of phenol formation (k_{2obs} in Figures 1 and 5) and the rate constant of Fe^{III}-(OOH) self-decay (Figures 2 and 5) are comparable and do not depend on [H_2O_2]. These observations indicate that self-decay of Fe^{III}(OOH) yields reactive intermediate that rapidly attacks the aromatic ring. To test this hypothesis, the reactivity of pre-generated Fe^{III}(OOH) was studied directly in a series of double-mixing experiments.

The rate of phenolate accumulation did not depend on the concentration of benzene added to a pre-generated Fe^{III}-(OOH) (Table S5 in the Supporting Information). Rate of hydroxylation also does not depend on the nature of substrate: when different substrates (benzene, chlorobenzene, toluene) were added to the pre-generated **2**, the rate constants of Fe^{III}–phenolate formation were nearly identical (Table S3 in the Supporting Information). Moreover, the rate of aromatic hydroxylation did not depend on the concentration of excess H_2O_2: Fe^{III}(OOH) was generated by mixing **1** and variable amounts of H_2O_2 (3, 10, and 20 equiv vs. **1**), followed by the addition of benzene at the maximum accumulation of Fe^{III}(OOH), and the rate constants of phenolate formation were equal in all of these experiments. All kinetic data suggest that Fe^{III}(OOH) does not directly attack the aromatic ring of the substrate, but this species decays into another species (presumably, Fe^{V}=O or Fe^{IV}=O), which rapidly hydroxylates the aromatic ring (Scheme 5).

Acetic acid facilitates Fe^{III}(OOH) decay in a concentration-dependent manner: larger amounts of acid lead to faster hydroperoxide decomposition (Figure S16 in the Supporting Information). Additionally, acetic acid accelerates the rate of Fe^{III}–phenolate formation (Figure 6), and the rate constants of phenolate formation and those of self-decay of **2** in the presence of one equivalent of acetic acid are comparable (Figure S17 in the Supporting Information). These data indicate that acetic acid accelerates the decay of Fe^{III}(OOH) into a reactive intermediate responsible for aro-

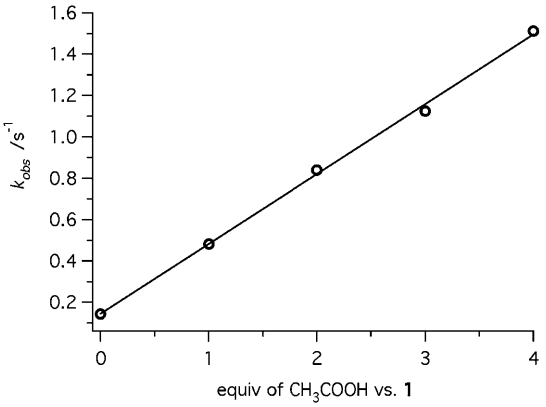

Figure 6. Rate constant of phenolate formation is directly proportional to [CH_3COOH] ([**1**] = 0.5 mM, [H_2O_2] = 5 mM, 560 equiv of benzene vs. 1, 20 °C, acetonitrile).

matic hydroxylation. Addition of acetic acid is known to increase catalytic activity of **1** in epoxidation and aliphatic C–H oxidation reactions.[1,7] We have also observed a somewhat increased yield of aromatic hydroxylation products in reactions of benzenes with **1**/H_2O_2 in the presence of acetic acid (Figure S18 in the Supporting Information).

Products of decomposition of Fe^{III}(OOH) and their role in hydroxylation reaction: Kinetic data suggest that decomposition of Fe^{III}(OOH) yields an active oxidant and acetic acid accelerates this process. Therefore we trapped and characterized the decay product of Fe^{III}(OOH) and probed its activity toward aromatic substrates.

We followed the decay of **2** by UV/Vis spectrophotometry and observed the formation of a green species **4** with λ_{max} = 740 nm (Figure S19 in the Supporting Information). This near-IR chromophore closely resembles low-spin L–Fe^{IV}=O complexes generated by O–O bond homolysis of L–Fe^{III}-(OOH) intermediates supported by several polyamine- or aminopyridine ligands (L) analogous to bpmen,[33] suggesting that **4** can also be formulated as an Fe^{IV}=O intermediate. This formulation is consistent with the EPR-silent nature of the green intermediate **4**: it was found that **2** decayed over 70 s ($k \approx 0.01\ s^{-1}$, RT) at room temperature without formation of any new EPR-active species (Figure S20 in the Supporting Information).

The chemical nature of **4** suggested alternative methods of generating this intermediate. Similarly to literature precedents,[12] **4** can be obtained faster and in higher yield from the reaction of **2** with acetic acid (Figure 7), or by adding a mixture of H_2O_2 and acetic acid directly to **1** (Figure 8). Acetic acid, added directly into EPR tube to a pre-generated **2**, accelerated decomposition of **2** into an EPR-silent species **4**, while **3** (which initially accompanied **4**—*g* values at 2.41, 2.17 and 1.90) remained intact (Figure 7, inset). The ESI-MS spectrum of the mixture of **1**/H_2O_2/CH_3COOH at

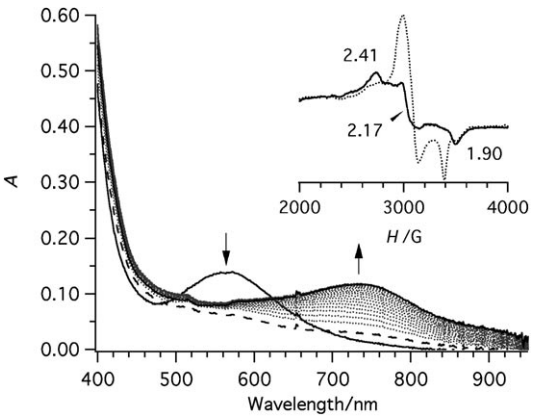

Figure 7. Stopped-flow time-resolved UV/Vis spectra of the reaction of Fe^{III}(OOH) with one equivalent of acetic acid. Fe^{III}(OOH) was pre-generated by mixing **1** (0.5 mM) and H_2O_2 (5 mM) at 20 °C in acetonitrile over 10 s (solid line, λ_{max} = 560 nm). Fe^{III}(OOH) decays quickly (2 s) upon addition of acetic acid (1 equiv vs. iron, dashed line) followed by slow (over 80 s) accumulation of Fe^{IV}=O (solid line, λ_{max} = 740 nm).[35] Inset shows EPR spectra of Fe^{III}(OOH) before (dotted line) and after (solid line) addition of acetic acid at room temperature.

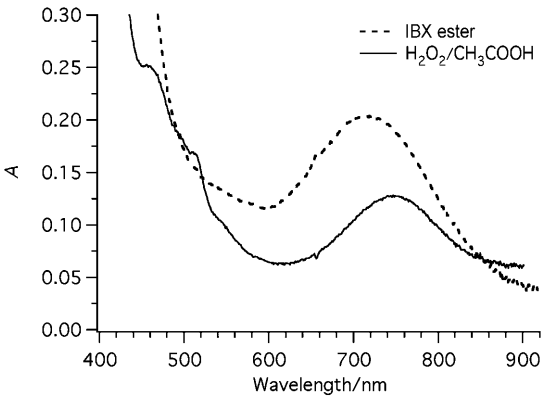

Figure 8. Spectra of green species **4** obtained upon mixing of **1** with IBX ester ([**1**] = 1 mM; [IBX ester] = 3.8 mM, acetonitrile, 10 °C) and **1** with H_2O_2/CH_3COOH ([**1**] = 1 mM, [H_2O_2] = 10 mM, [CH_3COOH] = 0.5 mM, acetonitrile, 20 °C).

room temperature shows peaks at m/z = 401, 425, 442 that correspond to $[Fe(bpmen)(O)+OAc]^+$, $[Fe(bpmen)+ClO_4]^+$, $[Fe(bpmen)(OH)+ClO_4]^+$ respectively (Figure S21 in the Supporting Information). Preliminary Mössbauer studies of the sample prepared by adding peracetic acid directly to **1** also confirms that the green species **4** has an Fe^{IV}=O center.[34]

Additionally, we used an alternative, H_2O_2-free method to directly generate the green species **4** from **1** and oxygen atom donors. The isopropyl ester of 2-iodoxybenzoic acid (IBX ester)[36] was recently developed as a stable, highly soluble source of oxygen atoms in organic oxidations. This reagent was also successfully used in metal-mediated oxidations catalyzed by phthalocyanin complexes.[37] We applied the IBX ester as an oxygen-atom transfer reagent in reactions that generate high-valent iron(IV)–oxo species. Upon mixing **1** and IBX ester (0.5–4 equiv vs. **1**) no purple species was observed, but instead a green species **4** formed, with an optical spectrum very similar to the spectra of the species generated from **1**, H_2O_2, and HOAc (Figure 8). The difference in spectra of the species **4** derived from **1**/IBX ester and **1**/H_2O_2/CH_3COOH can be attributed to the binding of HOAc or OAc to the Fe^{IV}=O center.[38]

To test the reactivity of the iron–oxo center, we generated bpmen–Fe^{IV}=O by mixing **1**, H_2O_2, and acetic acid at 20 °C. After **4** was formed in its maximum yield (60 s), benzene was added; however, only self-decay of **4** was observed. In a similar experiment, **4** was prepared by mixing **1** and IBX ester at 10 °C, addition of benzene (280 equiv vs. iron) did not result in the formation of the Fe^{III}–phenolate complex. It can be concluded that the Fe^{IV}=O intermediate **4** is unable to hydroxylate the aromatic ring, and cannot act as kinetically competent intermediate in aromatic hydroxylation with H_2O_2 promoted by **1**. We also used the stopped-flow methodology to measure rates of Fe^{IV}=O decay in the presence of toluene and without toluene and found that they are comparable (Figure S22 in the Supporting Information); therefore, bpmen–Fe^{IV}=O does not efficiently hydroxylate benzylic CH_3 groups.

Mechanistic insights into O–O bond cleavage in Fe^{III} peroxides supported by bpmen: Isotope-labeling experiments ($^{18}O/^{16}O$) are often useful in determining the mechanistic pathways of metal-assisted O–O bond cleavage. Incorporation of oxygen from water into the oxidation product requires the formation of Fe^{IV}=O or Fe^{V}=O species and $^{16}O/^{18}O$ exchange with solvent water prior to reaction with substrates.[39,40] In our system, hydroxylation experiments with labeled hydrogen peroxide ($H_2{}^{18}O_2$) in the presence of water ($H_2{}^{16}O$) show the incorporation of ^{16}O into phenol product: 19% of phenol contained ^{16}O and 81% of phenol contained ^{18}O. Hydroxylation of benzene with $H_2{}^{16}O_2$ in the presence of $H_2{}^{18}O$ led to 78% $H^{16}O$-C_6H_5 and 22% of $H^{18}O$-C_6H_5. The results of isotope-labeling studies are inconsistent with the mechanisms involving a direct attack of Fe^{III}(OOH) on the aromatic ring, because Fe^{III}-(OOH) cannot exchange with water. Similarly, ^{18}O-labeling studies showed some loss of the label when $H_2{}^{18}O_2$ was used as oxygen source for *cis*-dihydroxylation of naphthalene by naphthalene 1,2-dioxygenase,[41] thus implicating oxygen exchange between the active intermediate and water, and suggesting a reaction pathway that invokes Fe^{V}=O(OH) species. In another example,[31] a *cis*-dihydroxylation reaction of alkenes with hydrogen peroxide in the presence of $H_2{}^{18}O$ catalyzed by $[Fe^{II}(tpa)(CH_3CN)_2]^{2+}$ (tpa = tris(2-pyridylmethyl)-amine) showed incorporation of ^{18}O into product, which was rationalized by water-assisted formation of Fe^{V}=O(OH). Coordination of acetic acid to the iron–oxo moiety interfered with this water-assisted $^{18}O/^{16}O$ exchange, decreasing the incorporation of the ^{18}O from water in the products;[12,31] a similar effect was also observed in our experiments on benzene hydroxylation with **1**/H_2O_2/HOAc.

The $^{18}O/^{16}O$ scrambling in aromatic hydroxylations with H_2O_2 promoted by **1** implies that the observed peroxo intermediate, Fe^{III}(OOH), is not the sole oxidant in this reaction and thus should undergo either a heterolytic O–O bond cleavage that affords Fe^{V}=O, or a homolytic O–O bond cleavage to produce Fe^{IV}=O. In similar reactions, organic peroxide MPPH (2-methyl-1-phenyl-2-propyl hydroperoxide) has been widely used as a mechanistic probe to distinguish homolytic versus heterolytic cleavage of the alkylperoxide O–O bond.[42–45] Homolysis of RO–O bond would generate a Fe^{IV}=O species and a transient RO$^{\bullet}$ radical that decays into benzyl radical, eventually yielding benzyl alcohol under anaerobic conditions, or benzaldehyde in the presence of O_2 (Scheme 3). On the other hand, heterolytic cleavage of the O–O bond would generate Fe^{V}=O and 2-methyl-1-phenyl-2-propyl alcohol (MPPol). Analysis of organic products provides the information on the mechanism of O–O bond cleavage in oxidations with MPPH.

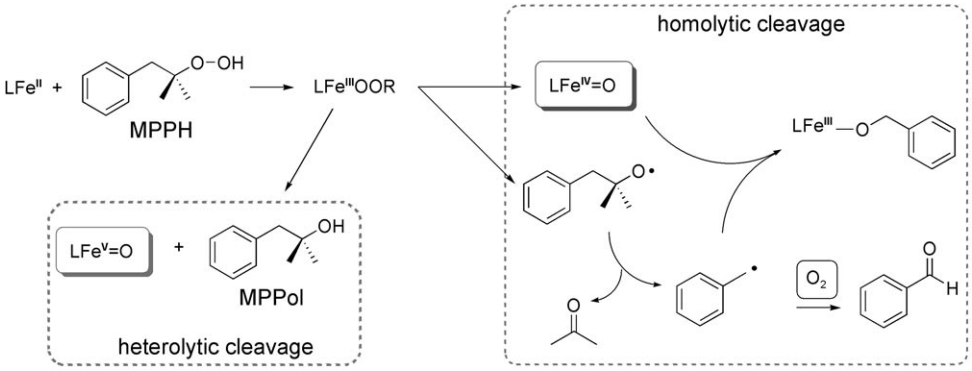

Scheme 3. Reaction of MPPH with iron center and products derived from MPPH.

Pure recrystallized MPPH reacted with **1**/benzene under aerobic conditions to yield mainly benzaldehyde, which indicated the O–O bond homolysis and the formation of Fe^{IV}=O (Scheme 3); the amount of MPPol, an indicator of O–O bond heterolysis, was small. Yield of phenol was low under these conditions (Figure 9a). In contrast, oxidation of benzene by MPPH in the presence of **1** and 0.5 equivalents of acetic acid resulted in significant increase in the yields of both MPPol and phenol (Figure 9b). These results are consistent with O–O bond heterolysis as a major pathway that generates a competent oxidant for benzene, implying that Fe^{V}=O is the active species in the hydroxylation reaction. Acetic acid catalyzes heterolytic O–O bond cleavage and the formation of Fe^{V}=O, therefore acetic acid dramatically increased the yield of MPPol and the yield of aromatic hydroxylation product when MPPH is used as oxidant.

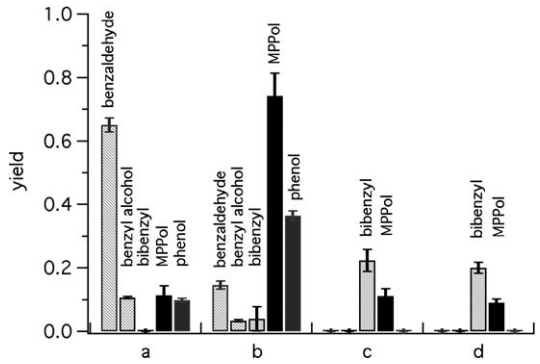

Figure 9. Product yields (in mol per 1 mol of Fe) and effects of acetic acid in aerobic reaction of benzene with **1**/MPPH (Scheme 3): a) [**1**] = 2 mM, 280 equiv of benzene vs. **1**, 1 equiv of MPPH; b) [**1**] = 2 mM, 280 equiv of benzene vs. **1**, 1 equiv of MPPH, 0.5 equiv of acetic acid; control experiments:[46] c) MPPH in acetonitrile (same amount as in a and b); d) MPPH and acetic acid (same amounts as in b). All samples were stirred for 30 min, then acetylated, products extracted with dichloromethane and analyzed by GCMS. Error bars show standard deviation.

H/D kinetic isotope effects in substrate oxidations with 1/H_2O_2: The mechanisms of interactions between the oxidant and the organic substrate can be evaluated by comparing

the relative rates of hydroxylation of deuterated and unlabeled substrates. While detailed calculations are necessary for thorough interpretation of H/D kinetic isotope effects, some qualitative conclusions can be derived from the direct analysis of the experimental data. In particular, C–H bond breakage (e.g., in a hydrogen-atom abstraction or direct insertion, Scheme 4 A,B) typically results in normal kinetic isotope effects (KIE > 1), but electrophilic attack on the aromatic ring accompanied by sp^2/sp^3 rehybridization often leads to small inverse kinetic isotope effects (Scheme 4 C,D).[47]

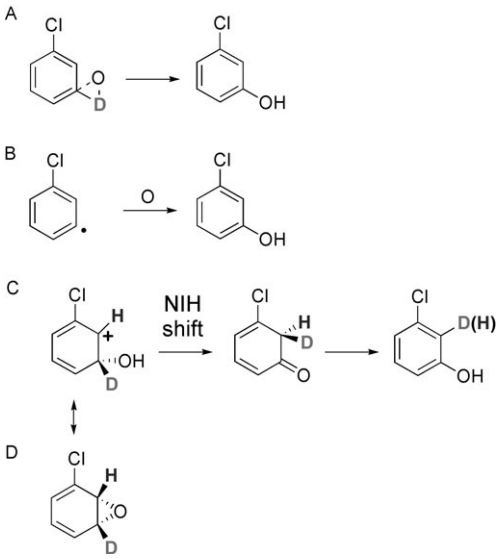

Benzene hydroxylation in the presence of **1**/H_2O_2 resulted in inverse KIE $k_H/k_D = 0.8$. The inverse kinetic isotope effect in benzene hydroxylation indicates a change in hybridization at a carbon bound to deuterium ($sp^2 \rightarrow sp^3$), which is consistent with an electrophilic addition to the aromatic ring or with an intermediate formation of epoxide.[48,49] The inverse H/D kinetic isotope effect is inconsistent with an abstraction–recombination sequence, which therefore can be excluded for aromatic hydroxylation with **1**/H_2O_2. Also toluene hydroxylation with H_2O_2 in the presence of **1** gave kinetic isotope effects of 0.7 for the aromatic ring hydroxylation and 1.3 for the methyl group hydroxylation. These data indicate that a hydrogen-atom abstraction is probably involved in benzylic hydroxylation of toluene, but not in the hydroxylation of the aromatic ring. Very similar values of H/D KIE in toluene hydroxylation were observed in the presence of acetic acid, indicating an electrophilic nature of the oxidant that attacks the aromatic ring under various reaction conditions. The differences in isotope effects observed for hydroxylation of the aliphatic chain and the aromatic ring suggest that two different mechanisms are utilized to oxidize these molecular fragments, although both processes (aliphatic and aromatic hydroxylation) may share the same metal-based oxidant. Similarly, previously reported hydroxylation of *p*-xylene catalyzed by toluene 4-monooxygenase, a non-heme iron enzyme, gave normal isotope effect (2.22) for methyl hydroxylation and inverse isotope effect (0.735) for aromatic hydroxylation.[49] P450 was also shown to give normal isotope effect (7–10) for benzylic hydroxylation of xylene, in agreement with an oxygen rebound mechanism; in contrast, aromatic hydroxylation of xylenes was characterized by an inverse isotope effect (0.83–0.94).[50]

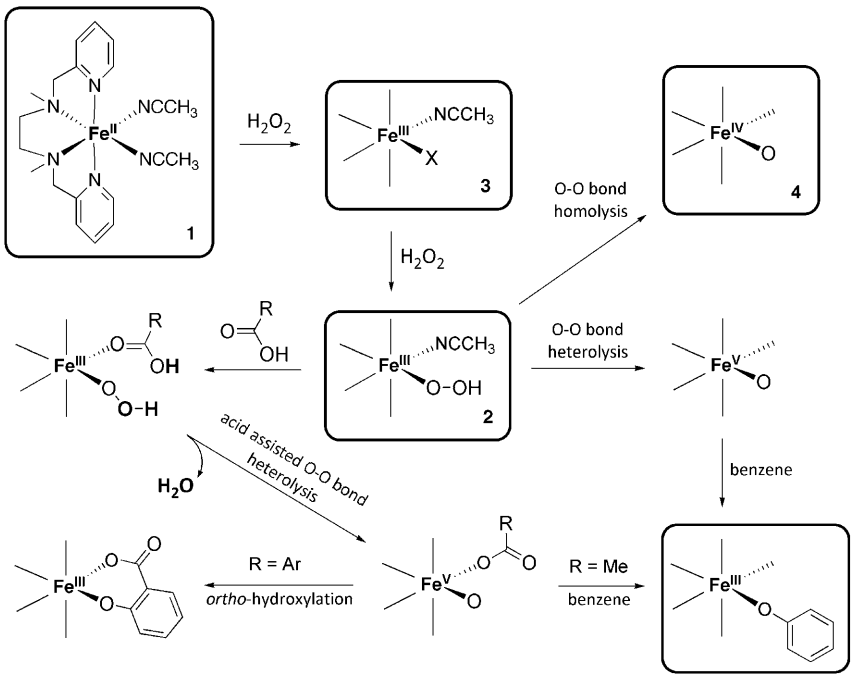

In addition to kinetic isotope effects, H/D migrations and rearrangements provide meaningful mechanistic information. In aromatic hydroxylations, a hydrogen-atom shift (the so-called NIH shift) is common for reactions that proceed through an electrophilic attack of the oxidant on the aromatic ring with subsequent rearrangement of the cationic intermediate to a ketone intermediate (Scheme 4C).[51] We observed a non-zero NIH shift for hydroxylation of 3,5-$^2H_2$-chlorobenzene and 2,4,6-$^2H_3$-chlorobenzene with **1**/H_2O_2; these results corroborate electrophilic addition to the aromatic ring (Table S6 in the Supporting Information).

The results obtained for aromatic hydroxylations with hydrogen peroxide in the presence of **1** are in line with a

number of related oxidations at the iron center that typically show a small inverse kinetic isotope effect, and agree with an electrophilic attack on the aromatic ring.[48,49,52–54]

Discussion

High activity of complex **1** in oxidation of organic substrates with hydrogen peroxide[2,7,12] made this complex a promising candidate for exploring intermolecular aromatic hydroxylation of substrates lacking directing groups. Similar to previously reported functional-group-assisted hydroxylation of benzoic acids, we now found that **1** is equally efficient in promoting hydroxylation of benzenes. Although biological aromatic hydroxylations can be catalyzed by mononuclear non-heme iron centers in pterin-dependent aromatic amino acid hydroxylases,[55] and by non-heme diiron centers in bacterial multicomponent monooxygenases (BMMs), such as methane and toluene monooxygenases,[56] synthetic biomimetic systems capable of hydroxylating unfunctionalized aromatic rings are still limited.[57] Aside from variations of classical Fenton reaction, which are usually non-selective and often low-yielding, iron phthalocyanines[58] and iron complexes with aminopyridine ligands[59] are among a handful of recent examples of non-porphyrin complexes reactive in intermolecular aromatic hydroxylations. Complex **1** promotes nearly quantitative conversion of aromatic hydrocarbons to phenolates at room temperature within several minutes, with H_2O_2 as the oxidant. Importantly, a range of substituted benzenes, including electron-poor substrates (such as chlorobenzene) readily undergoes hydroxylation with **1**/H_2O_2. However, strongly electron-withdrawing substituents (e.g., nitro groups) significantly decrease the yield of hydroxylated product. Despite high reaction rates in aromatic hydroxylation with **1**/H_2O_2, efficient catalysis is precluded by strong coordination of the phenolate products to the iron(III) center. This coordination, however, has two beneficial effects: it prevents overoxidation of phenols, thus greatly improving product selectivity, and it gives rise to intensely colored iron(III)–phenolate products, thus enabling spectrophotometric monitoring of the reaction progress. The latter feature was particularly useful for the present study, which was focused on identifying metal-based intermediates that are competent hydroxylating agents.

Plausible intermediates that were proposed for non-heme iron systems include Fe^{III}(OOH), Fe^{IV}=O, and some kind of a fleeting Fe^{V} species; all of these species were previously implicated in various iron-promoted oxidations, and most of them were spectroscopically observed for some non-heme iron complexes.[6] For intermolecular hydroxylations of non-functionalized aromatic compounds, a number of active non-heme iron reagents or catalysts is limited, and the active species in these systems were not identified.[60,61] Although Fe^{III}(OOH) was proposed to participate in aromatic hydroxylation,[61] the reactivity of this species was not studied in direct experiments. For example, anisol is hydroxylated with H_2O_2 in the presence of Fe^{II}–tpen (tpen = *N*,*N*,*N*′,*N*′-tetrakis(2-pyridylmethyl)ethane-1,2-diamine)) analogues, and hydroperoxo intermediates were proposed to be responsible for catalytic activity, but no specific experiments that support this hypothesis were described.[61] Pre-generated Fe^{III}OOH species supported by several aminopyridine ligands (including tris-picolylamine, tpa) were shown to be sluggish oxidants that did not react with olefins, sulfide, or phosphines[32] at low temperatures. However, very little information is available about Fe–bpmen-derived intermediates, therefore we developed methods to generate bpmen-supported Fe^{III}(OOH) in reasonable yield, and probed its reactivity under ambient conditions where high-yielding hydroxylation takes place.

Formation of the $[Fe^{III}(OOH)(bpmen)]^{2+}$ intermediate involved in hydroxylation was observed by stopped-flow kinetic measurements with spectrophotometric registration, by EPR spectroscopy, and by mass spectrometry. The yield of the Fe^{III}(OOH) intermediate significantly depends on temperature; counterintuitively, it can be generated in relatively high yield only at or near room temperature. Using stopped-flow techniques we established that $[Fe^{III}(OOH)(bpmen)]^{2+}$ does not directly attack aromatic substrates: reaction rates were independent on the concentration of benzene and on the nature of substituent on the aromatic ring. Also, ^{18}O-labeling experiments demonstrated that active intermediate responsible for aromatic hydroxylation exchanges with water and thus Fe^{III}(OOH) cannot be the sole oxidant. These results are in line with generally low oxidizing reactivity of Fe^{III}(OOH) intermediates.[62] A somewhat different situation was found for iron bleomycin (BLM), a natural antibiotic that causes oxidative DNA cleavage in the presence of iron and dioxygen.[63] Although earlier studies indicated nearly identical decay rates of activated BLM (ABLM) with and without substrate present,[64] the more recent study by Solomon and co-workers,[26] which took advantage of a distinct signature of ABLM in MCD spectra, provides evidence in favor of direct interaction between this Fe^{III}(OOH) intermediate and the substrate. Differences in reactivity of synthetic Fe^{III}(OOH) complexes (which are sluggish oxidants) compared to a natural system, ABLM, can be attributed, at least in part, to differences in spin states of iron(III), and to enzyme-like proximity effects due to bleomycin intercalation between the DNA base pairs.

Results presented herein, suggest that self-decomposition of Fe^{III}(OOH) generates an active species capable of oxidizing an aromatic substrate. Fe^{III}(OOH) can udergo heterolytic or homolytic O–O bond cleavage to produce Fe^{V}=O or Fe^{IV}=O respectively (Scheme 5). It is believed that mononuclear non-heme iron enzymes that hydroxylate aromatic substrates, pterin-dependent oxygenases (PheH, TyrH, TrpH), function by means of high-spin Fe^{IV}=O;[65] recently this intermediate was trapped in the reaction catalyzed by Tyrosine hydroxylase (TyrH) and characterized by rapid freeze–quench Mössbauer spectroscopy.[66] By now many synthetic Fe^{IV}=O complexes have been generated and characterized spectroscopically and, in several cases, crystallographically,[3–5] and in some cases, this species was able to carry out

an oxidation of organic substrates (cyclooctene,[67,68] cyclohexane,[43] thioanisole,[67] triphenylmethane,[60,69] alcohol,[60,70] anthracene[53]). Intramolecular, regioselective hydroxylation of the appended aromatic ring in reaction of $[Fe^{II}(6\text{-Ph-tpa})(CH_3CN)_2]^{2+}$ (6-Ph-tpa = tris(6-phenyl-2-pyridylmethyl)-amine) with *t*BuOOH also reportedly proceeds by means of a homolytic pathway that generates an Fe^{IV}=O species as a competent oxidant.[42] However, we recently showed that the tpa–Fe^{IV}=O intermediate does not hydroxylate benzoic acids.[2] In addition, an Fe^{IV}=O intermediate supported by a substituted TPEN did not oxidize anisole (although efficient anisole hydroxylation with H_2O_2 was promoted by this iron complex).[61] In the present work, we were able to generate, in high yield, an Fe^{IV}=O intermediate supported by bpmen, and confirmed that bpmen–Fe^{IV}=O does not hydroxylate aromatic rings. Similarly to iron(III)–hydroperoxo intermediates, the differences in reactivity of ferryl(IV) species in enzymes and in synthetic complexes can be attributed to different spin states of iron(IV)[63,71] (high spin in mononuclear non-heme iron enzymes,[72] and low spin in synthetic intermediates supported by aminopyridine ligands[73]), and by proximity effects in enzymes (and also in intramolecular ligand hydroxylations by iron(IV) species in synthetic systems).[42,63] An alternative mechanistic pathway that starts with O–O bond homolysis would utilize HO$^{\bullet}$ radicals in the hydrogen atom abstraction from the aromatic ring, immediately followed by an oxygen atom incorporation from the adjacent Fe^{IV}=O species. This scenario is inconsistent with inverse H/D kinetic isotope effects in aromatic hydroxylation (an electrophlic attack rather than a hydrogen atom abstraction must occur). In addition, use of an hydroxyl radical trap (galvinoxyl radical) did not effect the yields of phenols. Observed NIH shift also argues against HO$^{\bullet}$ radicals playing a major role in the aromatic ring hydroxylation.

We have shown that acetic acid facilitates decay of Fe^{III}-(OOH) and leads to faster Fe^{III}–phenolate formation, thus acetic acid promotes formation of reactive species responsible for aromatic hydroxylation. Moreover, acetic acid assisted O–O bond heterolysis of a mechanistic probe MPPH in the presence of **1** and benzene was accompanied by a significant growth in yields of hydroxylated products (phenolates), these results suggest that hydroxylation is performed by Fe^{V}=O species. Carboxylic acid assisted O–O bond heterolysis pathway, leading to an as-of-yet unobserved Fe^{V}=O oxidant, has been proposed[12] by Mas-Ballesté and Que in the efficient epoxidation of olefins by H_2O_2 in the presence of acetic acid and $[Fe^{II}(tpa)(CH_3CN)_2]^{2+}$, and it also appears to be a likely mechanism of regioselective benzoic acid hydroxylations.[2] Recently, another example of aromatic hydroxylation involving a proposed Fe^{V}=O intermediate was reported. Upon addition of CH_3CO_3H to a solution containing $[Fe^{II}(bqen)]^{2+}$ (bqen = *N*,*N*′-dimethyl-*N*,*N*′-bis(8-quinolyl)-ethane-1,2-diamine) and benzyl alcohol, aromatic ring was hydroxylated at the *ortho*-position.[60] Interestingly, the corresponding Fe^{IV}=O species did not hydroxylate aromatic ring, but produced benzaldehyde. The intermediate responsible for aromatic hydroxylation was found to rapidly exchange with $H_2{}^{18}O$ and was formulated as an Fe^{V}=O species. A similar oxidant has been proposed for the iron-catalyzed self-hydroxylation of aryl peroxyacids,[74] and for the intramolecular hydroxylation of the aromatic ring covalently appended to the analogue of **1**.[75] Although only one non-heme iron(V)–oxo complex has been directly observed at low temperature as a transient species and characterized by a variety of spectroscopic methods,[76] and recent (albeit preliminary)[77] EPR results suggested transient, low-yield generation of Fe^{V} from $[Fe(bpmen)]^{2+}$ and H_2O_2,[78] indirect evidence supporting participation of non-heme Fe^{V}–oxo intermediates in oxidations of alcohols,[79] olefins,[79–81] and arenes[60,75,82] continues to accumulate.

In summary, $[Fe(bpmen)(CH_3CN)_2][ClO_4]_2$ (complex **1**) is efficient in promoting hydroxylation of aromatic hydrocarbons with hydrogen peroxide, and the reaction is greatly accelerated by additions of carboxylic acids. The system reported herein is a rare example of an efficient aromatic hydroxylation with non-heme iron complex and hydrogen peroxide that allows for an unambiguous interpretation of the role of the Fe^{III}–hydroperoxo intermediates. A new bpmen–Fe^{III}(OOH) intermediate is definitely involved in the reaction pathway, but it does not attack the aromatic rings directly, generating a different, metal-based active oxidant instead. Another new intermediate, bpmen–Fe^{IV}=O, was generated and shown to be unreactive with aromatic substrates. An acid-assisted O–O bond heterolysis of coordinated peroxides is likely involved in the reaction pathway (Scheme 5). Inverse H/D kinetic isotope effects and the NIH shift in hydroxylations of selectively deuterated substituted benzenes imply an electrophilic attack of the aromatic ring by the oxidant and exclude a hydrogen atom abstraction as the key step in the hydroxylation pathways.

Experimental Section

All chemicals and solvents were purchased from Aldrich, Acros Organics or Fisher Scientific and were used without additional purification unless otherwise noted. $H_2{}^{18}O_2$ (90% isotopic purity, 2% solution in water) was obtained from ICON Isotopes, $H_2{}^{18}O$ (98%) was purchased from Cambridge Isotope Laboratories. Use of anhydrous HPLC grade acetonitrile is imperative in order to obtain Fe^{III}(OOH) intermediate. GCMS experiments were carried out using a Shimadzu GC-17 A gas chromatograph (Rtx-xLB column) with a GCMS-QP 5050 mass detector. Time-resolved spectra of rapid hydroxylation reactions were acquired with TgK Scientific (formerly Hi-Tech Schientific, Salisbury, Wiltshire, UK) SF-61DX2 cryogenic Stopped-flow system equipped with J&M Diode array (Spectralytics).

Materials: Isopropyl ester of 2-iodoxybenzoic acid (IBX ester),[36] *N*,*N*′-dimethyl-*N*,*N*′-bis(2-pyridylmethyl)ethane-1,2-diamine (bpmen)[83] and $[Fe(bpmen)(CH_3CN)_2](ClO_4)_2$ (**1**)[84] were prepared using published procedures. 2-Methyl-1-phenyl-2-propyl hydroperoxide (MPPH), generously provided by Prof. John Caradonna, was recrystallized from pentane (20 °C) prior to use until iodometric titration proved > 98% activity.[44] For iodometric titration solid KI (210 mg) was added to recrystallized MPPH (30 mg) dissolved in aqueous acetic acid (20 mL, 25% v/v). The reaction was allowed to proceed for 10 h in a sealed flask followed by quick titration of the resulting brown solution with $Na_2S_2O_3$ (0.1 M aqueous solution).

Determination of phenol yield using GCMS: Mixture of **1** with benzene in CH_3CN was prepared in a glove box. Hydrogen peroxide was prepared aerobically and delivered at room temperature; the resulting solution was stirred for 30 min for reaction to complete. Reaction mixtures were acetylated (0.1 mL of 1-methylimidazole and 1 mL of acetic anhydride) for 30 min followed by addition of 1 M HCl (2 mL) and extraction with dichloromethane (1 mL). The organic layer was washed with saturated aqueous $NaHCO_3$ (2 mL), water (2 mL) and finally dried over $MgSO_4$. Internal standard (nitrobenzene or naphthalene) was added prior to the extraction. Yields of hydroxylated products were established by GCMS relative to the internal standard and converted to absolute yields using a calibration curve with phenyl acetate and the corresponding standard, determined prior to each run. All experiments were run at least in triplicate, reported yields are average of these trials.

Determination of H/D KIE: An solution of **1** (5 mM) in acetonitrile and a 1:1 mixture of toluene/[D8]toluene (150 equiv each; the ratio of protio/deuterio isotopomers was analyzed by GCMS and adjusted to 1:1 if necessary) was prepared in a glove box. H_2O_2 (3 equiv vs. **1**) was added dropwise at room temperature and the mixture was left to react for 30 min. Products were acetylated and subjected to GCMS analysis; the amounts of the ^2H and ^1H products were quantified by integrating the peaks of their corresponding ions. The *o*-, *m*-, and *p*-cresols were well separated in the chromatogram; however, the GC peak from *meta* cresol partially overlapped with benzyl alcohol. Therefore we used an ion unique to benzyl alcohol (91 for protio and 98 for deutero) to determine KIE for the hydroxylation of CH_3 group; relatively low intensity of this peak limits the accuracy of KIE for benzylic hydroxylation. Additional details are provided in Supporting Information (Figure S24).

Stopped-flow experiments: Kinetic measurements were performed in the diode array mode using a stopped-flow instrument. Reactivity of **1** with hydrogen peroxide in the presence of benzene was studied in acetonitrile at 20 °C. In a single mixing experiment, an acetonitrile solution of **1** and benzene was prepared in a glove box and mixed with H_2O_2 in the stopped-flow. In a double mixing experiment **1** was mixed with H_2O_2, the reaction mixture was incubated to reach the highest yield of $Fe^{III}(OOH)$ (age time), followed by addition of benzene. The effect of acetic acid on hydroxylation rate was studied in a double mixing experiment, in which $Fe^{III}(OOH)$ was pre-generated by mixing **1** and H_2O_2 at 20 °C followed by addition of benzene with variable amounts of acetic acid (1–4 equiv vs. **1**). Concentrations of all reagents are reported in the figure captions for the onset of the reaction (after mixing). Kinetic parameters were determined in SPECFIT (global fitting), Kinetic Studio or IgorPro using single-exponential (A→B) or double exponential (A→B→C) models. Single-exponential fit was calculated to $A = A_{inf} + \Delta A \exp(-kt)$, in which A_{inf} is absorbance of the reaction mixture after reaction is complete, $\Delta A = A_0 - A_{inf}$; A_0 is initial absorbance. Similarly, double-exponential fit was calculated using $A = A_{inf} + \Delta A_1 \exp(-k_1 t) + \Delta A_2 \exp(-k_2 t)$. All experiments were run in at least triplicate and averaged rate constants are reported. The activation enthalpy and entropy for $Fe^{III}(OOH)$ formation were calculated from linear Arrhenius and Eyring plots.

Isotope-labeling studies: A mixture of **1** (2 mM) and benzene (280 equiv vs. **1**) was prepared in a glove box. In experiments with labeled hydrogen peroxide, $H_2{}^{18}O_2$ (11 μL, 0.53 M, 3 equiv vs. **1**) was added to the **1**/benzene mixture (1 mL) at room temperature. In an experiment with labeled water, $H_2{}^{18}O$ (11 μL, 98%) was added to solution of the **1**/benzene (1 mL) prior to the addition of H_2O_2 (60 μL of 0.1 M H_2O_2 diluted by CH_3CN from 70% stock solution). After 30 min the reaction mixture was subjected to GCMS analysis as described above.

EPR studies: Purple species **2** was generated directly in the EPR tube by mixing **1** (3 mM, 0.15 mL) with H_2O_2 (30 mM, 0.15 mL) in acetonitrile at room temperature. The tube was frozen immediately after all hydrogen peroxide was injected (5 s). Complex **2** decays fast when treated with acetic acid: Complex **2** was pre-generated in the EPR tube as described above and then acetic acid (1.5 mM, 0.11 mL, <0.5 equiv vs. iron) was injected into the tube and reaction quenched in liquid nitrogen (reaction time 5 s). All EPR spectra were acquired at 120 K. EPR spectra simulation were done using SimFonia (Bruker).

MPPH cleavage: O_2 was bubbled through anaerobically prepared solution of **1** (2 mM) and benzene (280 equiv vs. iron) in acetonitrile (1 mL) for 20 s followed by injection of MPPH (60 μL, 2 μmol, 1 equiv vs. iron) at room temperature. After addition of MPPH, solutions were stirred for ≈30 min and prepared for GCMS analysis as described above. When looking at the effects of H^+ on the reactivity, acetic acid (10 μL, 1 μmol, 0.5 equiv vs. iron) was added to **1**/benzene mixture before purging it with O_2.

Blank solutions containing only pure acetonitrile (1 mL) were treated same way as the **1**/benzene mixtures. Control samples with pure bibenzyl, benzyl alcohol acetate, benzaldehyde, 2-methyl-1-phenyl-2-propyl alcohol acetate (MPPol), phenyl acetate and nitrobenzene were run to find detector response for each product against nitrobenzene.

Acknowledgements

We thank Prof. Dr. L. Que, Jr. for fruitful discussion and Dr. Ivan V. Korendovych and Dr. Rubén Mas-Ballesté for critical reading of the manuscript. This work was supported by the US Department of Energy (Grant DE-FG02–06ER15799). The NMR facility, the ESI-MS spectrometer, and rapid kinetic instrumentation at Tufts were supported by the NSF (grants CHE-9723772, MRI CHE 0821508, MRI CHE 0320783, and CHE 0639138).

[1] M. C. White, A. G. Doyle, E. N. Jacobsen, *J. Am. Chem. Soc.* **2001**, *123*, 7194.
[2] O. V. Makhlynets, P. Das, S. Taktak, M. Flook, R. Mas-Balleste, E. V. Rybak-Akimova, L. Que Jr. , *Chem. Eur. J.* **2009**, *15*, 13171.
[3] J.-U. Rohde, J.-H. In, M. H. Lim, W. W. Brennessel, M. R. Bukowski, A. Stubna, E. Münck, W. Nam, L. Que Jr. , *Science* **2003**, *299*, 1037.
[4] J. England, Y. Guo, E. R. Farquhar, V. G. Young, Jr., E. Münck, L. Que Jr. , *J. Am. Chem. Soc.* **2010**, *132*, 8635.
[5] E. J. Klinker, J. Kaizer, W. W. Brennessel, N. L. Woodrum, C. J. Cramer, L. Que, Jr., *Angew. Chem.* **2005**, *117*, 3756; *Angew. Chem. Int. Ed.* **2005**, *44*, 3690.
[6] L. Que, Jr., W. B. Tolman, *Nature* **2008**, *455*, 333.
[7] M. S. Chen, C. White, *Science* **2007**, *318*, 783.
[8] S. Taktak, M. Flook, B. M. Foxman, L. Que, Jr., E. V. Rybak-Akimova, *Chem. Commun.* **2005**, 5301.
[9] L. Que, Jr., *J. Biol. Inorg. Chem.* **2004**, *9*, 684.
[10] I. V. Korendovych, S. V. Kryatov, E. V. Rybak-Akimova, *Acc. Chem. Res.* **2007**, *40*, 510.
[11] E. A. Duban, K. P. Bryliakov, E. P. Talsi, *Eur. J. Inorg. Chem.* **2007**, 852.
[12] R. Mas-Ballesté, L. Que Jr. , *J. Am. Chem. Soc.* **2007**, *129*, 15964.
[13] Although blue species decays over time this process is not due to overoxidation reaction, GCMS analysis showed that the blue solution (maximum accumulation of phenolate) and the yellow solution (1 h after the onset of the reaction) contain the same amount of phenol (Figure S2 in the Supporting Information).
[14] H. Marusawa, K. Ichikawa, N. Narita, H. Murakami, K. Ito, T. Tezuka, *Bioorg. Med. Chem.* **2002**, *10*, 2283.
[15] C. Kim, K. Chen, J. Kim, L. Que, Jr., *J. Am. Chem. Soc.* **1997**, *119*, 5964.
[16] M. Lubben, A. Meetsma, E. C. Wilkinson, B. Ferinda, L. Que, Jr., *Angew. Chem.* **1995**, *107*, 1610; *Angew. Chem. Int. Ed. Engl.* **1995**, *34*, 1512.
[17] P. Mialane, A. Nivorojkine, G. Pratviel, L. Azema, M. Slany, F. Godde, A. Simaan, F. Banse, T. Kargar-Grisel, G. Bouchoux, J. Sainton, O. Horner, J. Guilhem, L. Tchertanova, B. Meunier, J.-J. Girerd, *Inorg. Chem.* **1999**, *38*, 1085.
[18] B. Bernal, I. M. Jensen, K. B. Jensen, C. J. McKenzie, H. Toftlund, J.-P. Tuchagues, *J. Chem. Soc. Dalton Trans.* **1995**, 3667.
[19] K. B. Jensen, C. J. McKenzie, N. P. Nielsen, J. Z. Pedersen, H. M. Svendsen, *Chem. Commun.* **1999**, 1313.

[20] T. J. Mizoguchi, S. J. Lippard, *J. Am. Chem. Soc.* **1998**, *120*, 11022.
[21] V. Balland, F. Banse, E. Anxolabehere-Mallart, M. Ghiladi, T. A. Mattioli, C. Philouze, G. Blondin, J.-J. Girerd, *Inorg. Chem.* **2003**, *42*, 2470.
[22] A. J. Simaan, S. Dopner, F. Banse, S. Bourcier, G. Bouchoux, A. Boussac, P. Hildebrandt, J.-J. Girerd, *Eur. J. Inorg. Chem.* **2000**, 1627.
[23] D. Quiñonero, K. Morokuma, D. G. Musaev, R. Mas-Ballesté, L. Que, Jr., *J. Am. Chem. Soc.* **2005**, *127*, 6548.
[24] J.-J. Girerd, F. Banse, A. J. Simaan, *Struct. Bonding (Berlin)* **2000**, *97*, 145.
[25] R. M. Burger, S. B. Horwitz, J. Peisach, J. B. Wittenberg, *J. Biol. Chem.* **1979**, *254*, 12299.
[26] M. S. Chow, L. V. Liu, E. I. Solomon, *Proc. Natl. Acad. Sci. USA* **2008**, *105*, 13241.
[27] I. Lippai, R. S. Magliozzo, J. Peisach, *J. Am. Chem. Soc.* **1999**, *121*, 780.
[28] C. Nguyen, R. J. Guajardo, P. K. Mascharak, *Inorg. Chem.* **1996**, *35*, 6273.
[29] W. Nam, R. Ho, J. S. Valentine, *J. Am. Chem. Soc.* **1991**, *113*, 7052.
[30] X. Shan, L. Que Jr. , *J. Inorg. Biochem.* **2006**, *100*, 421.
[31] K. Chen, M. Costas, L. Que Jr. , *J. Chem. Soc. Dalton Trans.* **2002**, 672.
[32] M. J. Park, J. Lee, Y. Suh, J. Kim, W. Nam, *J. Am. Chem. Soc.* **2006**, *128*, 2630.
[33] Y. Zhou, X. Shan, R. Mas-Balleste, M. R. Bukowski, A. Stubna, M. Chakrabarti, L. Slominski, J. A. Halfen, E. Münck, L. Que, Jr., *Angew. Chem.* **2008**, *120*, 1922; *Angew. Chem. Int. Ed.* **2008**, *47*, 1896.
[34] R. Mas-Ballesté, E. Münck, L. Que, Jr., unpublished results.
[35] Acetic acid facilitates O–O bond cleavage of $Fe^{III}(OOH)$ (purple) and formation of very unstable active species that quickly converts into iron(III) complex (yellow), the later reacts with hydrogen peroxide (in excess) to produce $Fe^{IV}=O$. To test this hypothesis we generated $Fe^{III}(OOH)$ by mixing **1** and 1.5 equiv of H_2O_2 (stoichiometric amount) and then added acetic acid to the preformed **2**, as expected we saw a decay of $Fe^{III}(OOH)$ and very low yield of $Fe^{IV}=O$ (Figure S23 in the Supporting Information).
[36] V. V. Zhdankin, D. N. Litvinov, A. Y. Koposov, T. Luu, M. J. Ferguson, R. McDonald, R. R. Tykwinski, *Chem. Commun.* **2004**, 106.
[37] I. M. Geraskin, O. Pavlova, H. M. Neu, M. S. Yusubov, V. N. Nemykin, V. V. Zhdankin, *Adv. Synth. Catal.* **2009**, *351*, 733.
[38] J.-U. Rohde, A. Stubna, E. Bominaar, E. Münck, W. Nam, L. Que Jr. , *Inorg. Chem.* **2006**, *45*, 6435.
[39] M. S. Seo, J.-H. In, S. O. Kim, N. Y. Oh, J. Hong, J. Kim, L. Que Jr. , W. Nam, *Angew. Chem.* **2004**, *116*, 2471; *Angew. Chem. Int. Ed.* **2004**, *43*, 2417.
[40] B. Meunier, J. Bernadou, *Struct. Bonding (Berlin)* **2000**, *97*, 1.
[41] M. D. Wolfe, J. D. Lipscomb, *J. Biol. Chem.* **2003**, *278*, 829.
[42] I. M. Jensen, S. J. Lange, M. P. Mehn, E. L. Que, L. Que, Jr., *J. Am. Chem. Soc.* **2003**, *125*, 2113.
[43] T. L. Foster, J. Caradonna, *J. Am. Chem. Soc.* **2003**, *125*, 3678.
[44] G. T. Rowe, E. V. Rybak-Akimova, J. P. Caradonna, *Chem. Eur. J.* **2008**, *14*, 8303.
[45] P. A. MacFaul, K. U. Ignold, D. D. M. Wayner, L. Que Jr. , *J. Am. Chem. Soc.* **1997**, *119*, 10594.
[46] To check stability of MPPH during the work up and GCMS experiments we set up two control experiments containing 1) MPPH and 2) MPPH with equimolar amount of acetic acid. In both cases the main product was bibenzyl (product of benzyl radical coupling) with small amount of MPPol. For hydroxylation experiments we used one equivalent of MPPH to minmize any contribution of MPPH self-decomposition.
[47] R. P. Hanzlik, G. O. Shearer, *Biochem. Pharmacol.* **1978**, *27*, 1441.
[48] K. R. Korzekwa, D. C. Swinney, W. F. Trager, *Biochemistry* **1989**, *28*, 9019.
[49] K. H. Mitchell, C. E. Rogge, T. Gierahn, B. G. Fox, *Proc. Natl. Acad. Sci. USA* **2003**, *100*, 3784.
[50] R. P. Hanzlik, K.-H. J. Ling, *J. Am. Chem. Soc.* **1993**, *115*, 9363.
[51] D. R. Boyd, J. W. Daly, D. M. Jerina, *Biochemistry* **1972**, *11*, 1961.
[52] M.-J. Kang, W. J. Song, A.-R. Han, Y. S. Choi, H. G. Jang, W. Nam, *J. Org. Chem.* **2007**, *72*, 6301.
[53] S. P. de Visser, K. Oh, A.-R. Han, W. Nam, *Inorg. Chem.* **2007**, *46*, 4632.
[54] G. R. Moran, A. Derecskei-Kovacs, P. J. Hillas, P. F. Fitzpatrick, *J. Am. Chem. Soc.* **2000**, *122*, 4535.
[55] P. C. A. Bruijnincx, G. van Koten, R. J. M. Klein Gebbink, *Chem. Soc. Rev.* **2008**, *37*, 2716.
[56] L. J. Murray, S. J. Lippard, *Acc. Chem. Res.* **2007**, *40*, 466.
[57] D. A. Alonso, C. Nájera, I. M. Pastor, M. Yus, *Chem. Eur. J.* **2010**, *16*, 5829.
[58] E. V. Kudrik, A. B. Sorokin, *Chem. Eur. J.* **2008**, *14*, 7123.
[59] A. Thibon, J.-F. Bartoli, R. Guillot, J. Sainton, M. Martinho, D. Mansuy, F. Banse, *J. Mol. Catal. A* **2008**, *287*, 115.
[60] J. Yoon, S. A. Wilson, Y. K. Jang, M. S. Seo, K. Nehru, B. Hedman, K. O. Hodgson, E. Bill, E. I. Solomon, W. Nam, *Angew. Chem.* **2009**, *121*, 1283; *Angew. Chem. Int. Ed.* **2009**, *48*, 1257.
[61] A. Thibon, J.-F. Bartoli, S. Bourcier, F. Banse, *Dalton Trans.* **2009**, 9587.
[62] E. V. Rybak-Akimova in *Physical Inorganic Chemistry* (Ed.: A. Bakac), Wiley, Hoboken, **2010**, pp. 109.
[63] E. I. Solomon, S. D. Wong, L. V. Liu, A. Decker, M. S. Chow, *Curr. Opin. Chem. Biol.* **2009**, *13*, 99.
[64] R. M. Burger, J. Peisach, S. B. Horwitz, *J. Biol. Chem.* **1981**, *256*, 11636.
[65] E. G. Kovaleva, J. Lipscomb, *Nat. Chem. Biol.* **2008**, *4*, 186.
[66] B. E. Eser, E. W. Barr, P. A. Frantom, L. Saleh, J. M. Bollinger, C. Krebs, P. F. Fitzpatrick, *J. Am. Chem. Soc.* **2007**, *129*, 11334.
[67] M. H. Lim, J.-U. Rohde, A. Stubna, M. R. Bukowski, M. Costas, R. Y. N. Ho, E. Münck, W. Nam, L. Que Jr. , *Proc. Natl. Acad. Sci. USA* **2003**, *100*, 3665.
[68] M. Martinho, F. Banse, J.-F. Bartoli, T. Mattioli, P. Battioni, O. Horner, S. Bourcier, J.-J. Girerd, *Inorg. Chem.* **2005**, *44*, 9592.
[69] J. Kaizer, E. J. Klinker, N. Y. Oh, J.-U. Rohde, W. J. Song, A. Stubna, J. Kim, E. Münck, W. Nam, L. Que, Jr., *J. Am. Chem. Soc.* **2004**, *126*, 472.
[70] N. Y. Oh, Y. Suh, M. J. Park, M. S. Seo, J. Kim, W. Nam, *Angew. Chem.* **2005**, *117*, 4307; *Angew. Chem. Int. Ed.* **2005**, *44*, 4235.
[71] G. Xue, R. De Hont, E. Münck, L. Que Jr. , *Nat. Chem.* **2010**, *2*, 400.
[72] J. M. Bollinger, Jr., C. Krebs, *J. Inorg. Biochem.* **2006**, *100*, 586.
[73] W. Nam, *Acc. Chem. Res.* **2007**, *40*, 522.
[74] N. Y. Oh, M. S. Seo, M. H. Lim, M. B. Consugar, M. J. Park, J.-U. Rohde, J. Han, K. M. Kim, J. Kim, L. Que, Jr., W. Nam, *Chem. Commun.* **2005**, 5644.
[75] A. Nielsen, F. B. Larsen, A. D. Bond, C. J. McKenzie, *Angew. Chem.* **2006**, *118*, 1632; *Angew. Chem. Int. Ed.* **2006**, *45*, 1602.
[76] F. T. de Oliveira, A. Chanda, D. Banerjee, X. Shan, S. Mondal, L. Que, Jr., E. Bominaar, E. Münck, T. J. Collins, *Science* **2007**, *315*, 835.
[77] We have not been able to trap the intermediate described in the paper.
[78] O. Y. Lyakin, K. P. Bryliakov, G. J. P. Britovsek, E. P. Talsi, *J. Am. Chem. Soc.* **2009**, *131*, 10798.
[79] S. H. Lee, J. H. Han, H. Kwak, E. Y. Lee, H. J. Kim, J. H. Lee, C. Bae, S. N. Lee, Y. Kim, C. Kim, *Chem. Eur. J.* **2007**, *13*, 9393.
[80] K. Chen, M. Costas, J. Kim, A. K. Tipton, L. Que Jr. , *J. Am. Chem. Soc.* **2002**, *124*, 3026.
[81] A. Company, Y. Feng, M. Güell, X. Ribas, J. M. Luis, L. Que, Jr., M. Costas, *Chem. Eur. J.* **2009**, *15*, 3359.
[82] Y. Feng, C. Ke, G. Xue, L. Que Jr. , *Chem. Commun.* **2009**, 50.
[83] S. Poussereau, G. Blondin, M. Cesario, J. Guilhem, G. Chottard, F. Gonnet, J.-J. Girerd, *Inorg. Chem.* **1998**, *37*, 3127.
[84] K. Chen, L. Que Jr. , *Chem. Commun.* **1999**, 1375.

Received: September 6, 2010
Published online: November 29, 2010

